

Relations between the Photoluminescence Efficiency of CdTe Nanocrystals and Their Surface Properties Revealed by Synchrotron XPS

Holger Borchert,^{*,†} Dmitri V. Talapin,[†] Nikolai Gaponik,[†] Colm McGinley,[‡] Sorin Adam,[‡] Arun Lobo,[‡] Thomas Möller,[‡] and Horst Weller[†]

Institute of Physical Chemistry, University of Hamburg, Bundesstr. 45, 20146 Hamburg, Germany, and Hamburger Synchrotronstrahlungslabor HASYLAB at DESY, Notkestr. 85, 22603 Hamburg, Germany

Received: May 10, 2003

The surface of colloiddally prepared CdTe nanocrystals capped with thioglycolic acid has been studied by photoelectron spectroscopy with tunable synchrotron radiation excitation. Colloiddally prepared CdTe nanocrystals possess photoluminescence properties which depend on the growth conditions. Two samples of the same particle size prepared at different net growth rates were investigated. The nanocrystals which were slowly grown in a dynamic equilibrium of growth and dissolution present a much higher photoluminescence quantum yield. We have performed a photoemission study in order to reveal if there are structural differences at the nanocrystal surface which might explain the observed differences in the photoluminescence efficiency. Significant differences are indeed observed in high-resolution spectra of the Te 4d and Te 3d level. In contrast to the highly luminescent nanocrystals, the lowly luminescent particles present a large amount of Te surface sites. A structure model is proposed which allows explanation of the differences in the luminescence efficiency.

1. Introduction

Most of the colloidal syntheses of semiconductor nanocrystals are based on the Ostwald ripening phenomenon. The formation of nanocrystals in solution is a dynamic process. After nucleation, further particle growth occurs via dissolution of small clusters in favor of the growth of larger particles. At any stage of growth in an ensemble of nanocrystals with a size distribution, to each particle size corresponds a specific ratio between growth and dissolution rates. This is illustrated by Figure 1a which shows the size distribution of an ensemble of nanocrystals at a specific moment during the preparation. For the large particles in the ensemble, the growth rate exceeds the rate of dissolution so that a positive net growth rate is obtained. For the small particles, the net growth rate is negative and they release monomer, i.e., molecular species containing the elements of the semiconductor compound in question, for further growth of the larger particles.

Approximately in the middle of the size distribution, there always exists a fraction of particles with equal rates of growth and dissolution. The nanocrystals' dissolution occurs preferably from surface sites having the highest energy (defects, kinks, etc.). On the other hand, monomers tend to occupy the energetically most favorable positions at the surface. The best conditions for the elimination of surface defects are given at a net growth rate close to zero. Note the dynamic nature of the process: when the whole ensemble of nanoparticles evolves in time, the particle size corresponding to zero net growth rate is also shifting. The distribution of the growth and dissolution rates during the formation of semiconductor nanocrystals has been studied theoretically by Talapin et al.¹

The conditions of growth are important for physical and chemical properties such as the photoluminescence efficiency

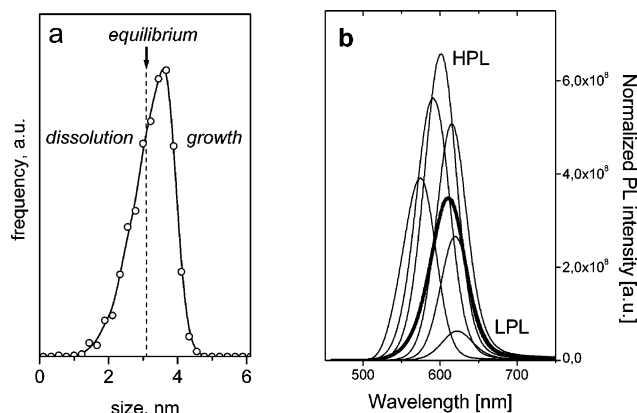


Figure 1. (a) Distribution of the rates of growth and dissolution in an ensemble of nanocrystals. (b) Photoluminescence spectra of as-prepared CdTe nanocrystals (thick curve) and fractions of this ensemble with narrow size distributions (thinner curves). The various fractions of the ensemble present drastic differences in the luminescence efficiency.

(PL efficiency) of semiconductor nanocrystals. Detailed studies of InAs,¹ CdSe,¹ and CdTe^{1,2} nanocrystals have revealed that the size fractions corresponding to very low net growth rates, i.e., when growth and dissolution are in an equilibrium, possess the highest photoluminescence quantum efficiencies and the best photostability. Those particles are supposed to have a highly ordered surface. In contrast, the nanocrystals grown under conditions far away from the equilibrium of growth and dissolution are supposed to possess a more rough surface with various defects giving rise to nonradiative recombination pathways.¹

Figure 1b illustrates the distribution of the photoluminescence efficiency within the crude solution of as-prepared CdTe nanocrystals. The curve plotted as a thick line is the luminescence spectrum of an ensemble of as-prepared CdTe nanocrystals. This spectrum represents the sum of the luminescence of

* Corresponding author. Fax: +49-40-42838-3452. E-mail: Holger_Borchert@public.uni-hamburg.de.

[†] Institute of Physical Chemistry, University of Hamburg.

[‡] Hamburger Synchrotronstrahlungslabor HASYLAB at DESY.

all particles in the ensemble. The ensemble can be divided into a series of fractions with narrow size distributions. The thinner curves in Figure 1b are normalized luminescence spectra of fractions with gradually changing particle size. The decomposition clearly shows that the quantum efficiency varies within the ensemble. The highest photoluminescence is observed for the size fraction which corresponds to the equilibrium of growth and dissolution.

These examples show that the dynamic growth process plays an important role in defining the nanocrystals' properties such as the photoluminescence efficiency. For nanocrystals possessing a large surface-to-volume ratio those properties are generally related to the surface structure. Hence it is essential to investigate the influence of the growth process on the surface structure and the implications on the nanocrystals' properties. A very powerful method for surface structure studies is photoelectron spectroscopy, especially with the use of tunable synchrotron radiation. Tuning the excitation energy influences the kinetic energy of the generated photoelectrons. And because of the well-known dependence of the mean free path length on the photoelectron kinetic energy,³ tuning the excitation energy means to vary the sampling depth. On the basis of this principle, it is possible to distinguish between atoms in the interior and atoms at the surface of a sample.

Investigations of CdS,^{4–6} ZnS,⁷ CdSe,⁸ and InAs⁹ nanocrystals are some examples for surface structure studies of semiconductor nanocrystals by high-resolution photoelectron spectroscopy. Furthermore, composite nanocrystals such as CdSe/ZnS⁸ core-shell or CdS/HgS/CdS¹⁰ quantum dot quantum well nanocrystals have been studied by synchrotron XPS.

In this study, we used photoelectron spectroscopy with tunable synchrotron radiation to investigate how the net growth rate influences the surface structure of CdTe nanocrystals capped with thioglycolic acid (TGA). The aim was to reveal if there are structural differences which can explain the observed differences in photoluminescence efficiency between nanocrystals present in the same portion of crude solution but corresponding to different net growth rates. A rather similar type of question has already been addressed by Zhang and Yang in a study of 3-mercaptopropionic acid-stabilized CdTe nanocrystals by photoelectron spectroscopy with Mg K α radiation.¹¹ They emphasized that effective surface passivation by the formation of cadmium–thiol complexes at the surface was found to be the origin of high photoluminescence quantum yields.¹¹ The use of synchrotron radiation in our investigation enables us to acquire high-resolution spectra which can provide more detailed and additional information.

2. Experimental Section

2.1. Preparation of CdTe Nanocrystals. CdTe nanocrystals stabilized with thioglycolic acid (TGA) have been prepared using a procedure described earlier.² Briefly, Cd(ClO₄)₂·6H₂O is dissolved in water and TGA is added under stirring. Next, an adjustment of the pH to appropriate values is achieved by dropwise addition of NaOH. After deaeration of the solution by N₂ bubbling, H₂Te gas is passed through the solution, and CdTe precursors are formed. Under reflux, the nanocrystals are grown to their final size.²

Portions of CdTe nanocrystals of different sizes were taken from the crude solution at different refluxing times. Each portion of crude solution was divided into a series of fractions with narrowed size distribution by a size-selective precipitation technique.²

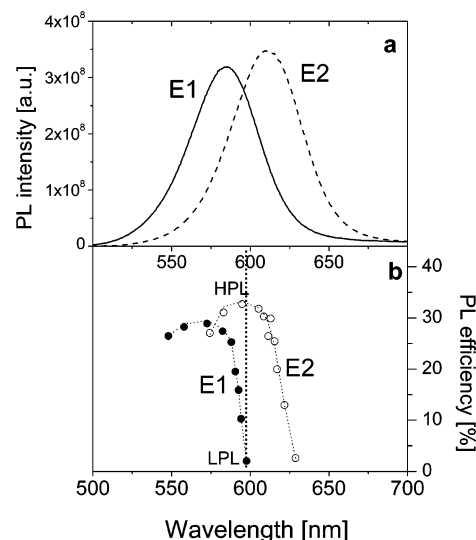


Figure 2. Photoluminescence spectra of the crude solution of CdTe nanocrystals (a). Spectra of the same ensemble are shown after two different times of refluxing where the dashed curve “E2” corresponds to a longer refluxing time. Part (b) shows the quantum efficiency of monodispersed fractions of portions of the ensembles “E1” and “E2”. The lowly luminescent fraction “LPL” of the ensemble “E1” has the same particle size as the highly luminescent fraction “HPL” of the ensemble “E2”.

Figure 2 illustrates the influence of the refluxing time on the optical properties of the ensemble of nanocrystals. Figure 2a shows luminescence spectra of the crude solution after two different times of refluxing. The spectra belong to the same ensemble of nanocrystals, but E2 corresponds to a longer time of refluxing (21 h) than E1 (6 h 15 min). Upon refluxing, the spectrum shifts toward higher wavelengths due to the growth of the nanocrystals by Ostwald ripening. Figure 2b shows the photoluminescence efficiency of fractions with narrow size distributions which have been separated from portions of the ensembles E1 and E2. Due to the evolution of the optical properties upon refluxing, it is possible to obtain fractions with the same particle size but with completely different luminescence efficiencies. The lowly luminescent fraction, LPL, of the ensemble E1 has the same particle size as the highly luminescent fraction HPL of the ensemble E2. This is a result of the temporal evolution of the distribution of the rates of growth and dissolution.

For the photoemission study, two fractions of TGA-stabilized CdTe samples have been prepared which are of the same particle size, but which have been grown at different net growth rates. The sample grown at conditions far away from the equilibrium of growth and dissolution has a very low photoluminescence quantum yield and is named “lowly luminescent sample” in the following discussion. The sample grown at conditions close to the equilibrium has a high photoluminescence efficiency. This sample is named “highly luminescent sample” in the following discussion.

Another point of special interest is the behavior of the sulfur from the organic stabilizer in the reaction mixture. It has been shown that the thiol stabilizer can partly hydrolyze under prolonged reflux which leads to a partial incorporation of S into the CdTe lattice.^{2,12} In this context, it has been supposed that the sulfur is mainly concentrated at the nanocrystal surface and that there is a gradient of sulfur content into the core of the particles.

2.2. Photoelectron Spectroscopy. Photoelectron spectroscopy was performed at beamline BW3 at HASYSLAB/DESY in

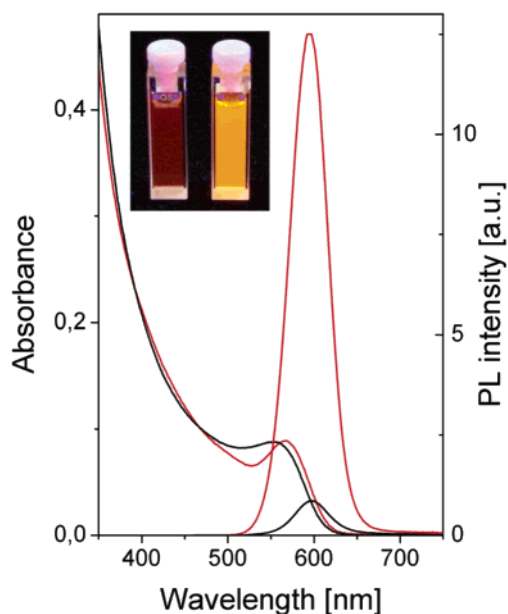


Figure 3. Normalized absorption and fluorescence spectra of the highly (red line) and lowly (black line) luminescent CdTe nanocrystals. The inset shows a photograph of the two samples under UV irradiation.

Hamburg, Germany. Synchrotron radiation has been tuned in the energy range from 100 to 1200 eV, and an Omicron EA 125 hemispherical energy analyzer has been used for acquiring the photoemission spectra. CdTe nanocrystals were deposited from aqueous solution on Au foils. A special technique was necessary to prevent charging of the samples. When an aqueous drop is simply placed on the gold, it does not spread out and dries only very slowly. Agglomerations of nanocrystals on the substrate and charging problems are the consequence. To overcome these difficulties, we have mixed the aqueous solutions of nanocrystals with acetone before deposition. The drops spread out better and dried more quickly so that more uniform films of nanocrystals could be achieved. Additionally, we worked with low concentrations of nanocrystals on the substrate in order to avoid agglomerations. With these precautions, no charging of the samples was observed.

Because of the monochromator characteristics, the total experimental resolution depends on the excitation energy. At a photon energy of 100 eV, an experimental resolution of about 130 meV could be achieved. At excitation energies around 600 eV and around 1200 eV, the resolution was limited to about 400 meV and to about 800 meV, respectively.

3. Optical Characterization of the CdTe Nanocrystals and Powder X-ray Diffraction

Figure 3 shows normalized absorption and fluorescence spectra of the highly and lowly luminescent CdTe samples selected for the photoemission study. The positions of the absorption and luminescence maxima are approximately the same for both samples. So the two samples contain nanocrystals of practically the same particle size. According to literature data on the size-dependent shift of the first absorption maximum,^{11,13} the diameter is approximately 3.4–3.6 nm.

The normalized luminescence spectra show a drastic difference between the two samples. The quantum efficiency is ~2% for the lowly and ~30% for the highly luminescent CdTe nanocrystals. This dramatic difference in photoluminescence efficiency can also be seen in the photograph presented in Figure 3.

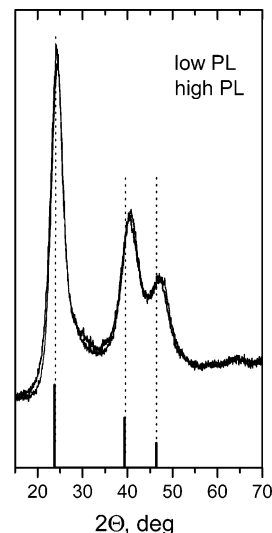


Figure 4. Powder X-ray diffractograms of highly and lowly luminescent CdTe nanocrystals of the same size. The line spectrum corresponds to the cubic phase of bulk CdTe.

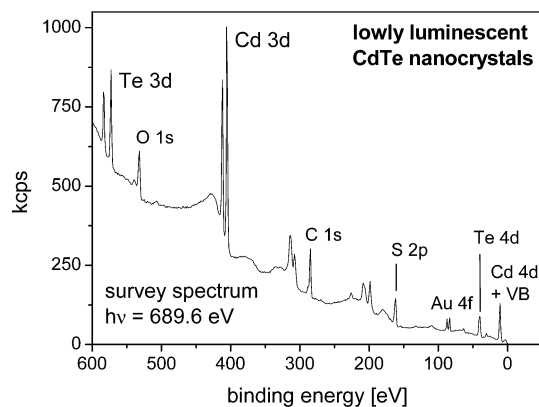


Figure 5. XPS overview spectrum of the lowly luminescent CdTe nanocrystals.

Powder X-ray diffraction shows that both HPL and LPL samples have the same crystallinity (cf. Figure 4). Therefore the differences in luminescence must be due to different surface properties which are studied in the following by photoelectron spectroscopy.

4. High-Resolution Photoelectron Spectroscopy

4.1. Overview Spectra. Figure 5 shows an overview spectrum of the lowly luminescent CdTe nanocrystals recorded at an excitation energy around 700 eV. Different Cd and Te core levels can be seen. Furthermore, carbon, oxygen, and sulfur from the organic ligands and a Au signal from the substrate show up. The Au 4f_{7/2} level at 84.0 eV has been used for calibration of the energy scale. In our study we focused on the Cd 3d, Te 3d, Te 4d, and S 2p levels. The Cd 4d level has a binding energy of about 10 eV and has not been studied here, because it is quite close to the valence band and therefore less reliable to analyze. Overview spectra of the highly luminescent CdTe nanocrystals (not shown) present the same core levels.

4.2. Study of the Cd 3d Level. Spectra of the Cd 3d level have been recorded at a series of excitation energies in the range from 460 to 630 eV. Figure 6 shows Cd 3d_{5/2} spectra recorded with high surface sensitivity for the highly (a) and lowly (b) luminescent CdTe nanocrystals. Using a combined polynomial and Shirley type background function, the spectrum (Figure 6a) of the highly luminescent nanocrystals is well fitable with one

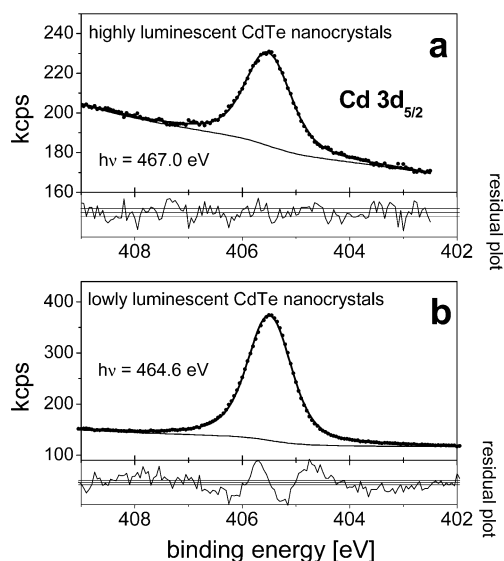


Figure 6. High-resolution Cd 3d_{5/2} spectra of the highly (a) and lowly (b) luminescent CdTe nanocrystals.

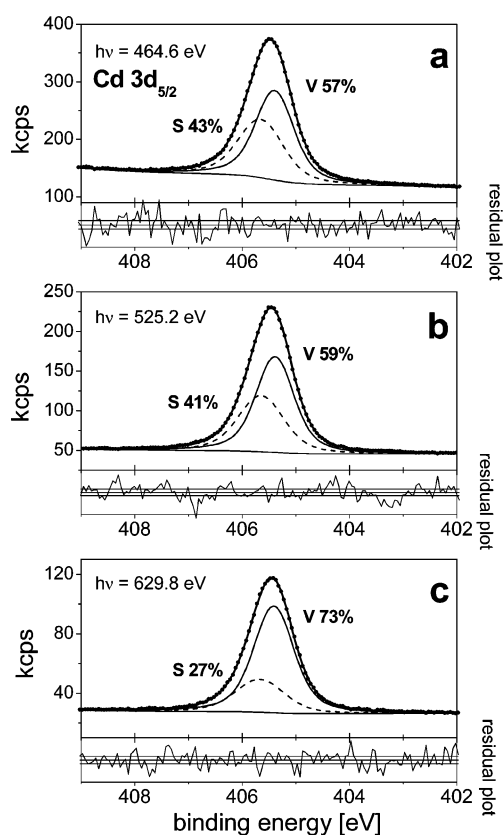


Figure 7. High-resolution Cd 3d_{5/2} spectra of the lowly luminescent CdTe nanocrystals fitted with two Voigt functions. The surface sensitivity decreases from (a) to (c).

single Voigt function. The binding energy of 405.5 eV is in good accordance with literature values for bulk CdTe.¹⁴ The Lorentzian and Gaussian widths are 0.48 and 0.73 eV in the presented fit.

In contrast, the residual of the fit of the spectrum presented in Figure 6b shows considerable deficiencies. Adequate fitting of the spectra of the lowly luminescent CdTe nanocrystals requires two Voigt functions. The corresponding fits are presented in Figure 7. The shift between the two components turned out to be quite small and of the order of the experimental resolution. By consequence, unambiguous fitting is delicate, and

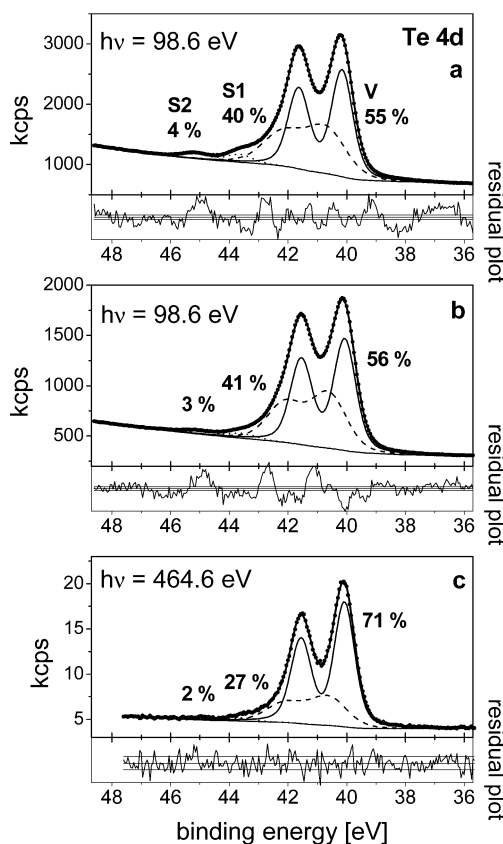


Figure 8. High resolution Te 4d spectra of the lowly luminescent CdTe nanocrystals at a surface-sensitive (a) and a more volume-sensitive energy (c). (b) is a repetition of (a) at a late stage of the experiment to check for charging or radiation damage.

especially relative peak intensities are quite sensitive to slight variations of the parameters. To enable a comparison of the relative intensities at different excitation energies, the parameters have been fixed to the average values of 0.4 eV for the Lorentzian width and 0.26 eV for the shift between the two components.

The relative intensity of the component labeled “V” increases with respect to the relative intensity of the component “S” when the excitation energy and thus the sampling depth is increased. Therefore we can assign the component “V” to atoms in the interior and the component “S” to atoms at the surface of the nanocrystals.

Two different reasons are to be considered for why a second component could not be resolved in the case of the highly luminescent nanocrystals. One possible reason is simply the difference in the quality of the data. The spectra of the lowly luminescent sample had a higher count rate. The reduction of the noise makes it easier to resolve distinct components. Another reason might be related to the sample structure. As mentioned earlier, one should expect that the lowly luminescent CdTe nanocrystals possess a rougher surface. A surface component should therefore be more pronounced in the case of the lowly luminescent nanocrystals. So the presence or absence of an observable surface component might also be understood as a hint for differences in the surface roughness.

4.3. Study of the Te 4d Level. Spectra of the Te 4d level have been recorded at a series of excitation energies in the range from 100 to 630 eV. Figure 8 shows high-resolution spectra of the lowly luminescent CdTe sample. The spectra have been fitted with a minimum number of Voigt functions where again a combined polynomial and Shirley type function has been used to take care of the steplike increase of the background. Three

spin-orbit split doublets of Voigt functions, labeled “V”, “S1”, and “S2”, were necessary to achieve consistent fits of all spectra in acceptable quality. The spin-orbit splitting was found to be 1.48 ± 0.01 , in agreement with literature values.¹⁵ The Lorentzian width was constrained to be identical for all components and turned out to be 0.3 eV, also in agreement with studies of bulk CdTe.^{16,17} While the spectra recorded at low excitation energy required values for the branching ratio of up to 0.77, at higher energies the normal value for d levels of 0.67 was found. Similar observations were made in various studies of bulk CdTe.^{15,17}

Figure 8a shows a spectrum recorded at a surface-sensitive energy. It has been recorded at an early stage of the experiment. To check for charging or radiation damage, some spectra have been recorded again under identical experimental conditions at the end of the measurements. The spectrum presented in Figure 8b is such a repetition spectrum of Figure 8a at a late stage of the experiment and shows that no substantial changes occurred.

Figure 8c shows a spectrum recorded at higher excitation energy, i.e., when the interior of the nanocrystals contributes more strongly to the spectra. At higher photon energy the relative intensity of the component “V” increases compared to the components “S1” and “S2”. Therefore, the component “V” can be assigned to Te atoms in the interior of the nanocrystals, whereas the components “S1” and “S2” correspond to surface Te atoms.

This assignment is also reasonable with respect to the widths of the components. For the fit presented in part a of Figure 8 the Gaussian widths are 0.69, 1.45, and 0.84 eV for the components “V”, “S1”, and “S2”, respectively. Slightly different surface sites lead to an additional broadening of the surface components with respect to the volume component. A detailed discussion of factors leading to inhomogeneous broadening of core level spectra in the particular case of nanocrystals is given in a study of CdSe nanocrystals.⁸

The $4d_{5/2}$ sublevel of the component “V” has a binding energy of 40.1 eV, in good accordance with values for the corresponding level in studies of bulk CdTe.¹⁸ The surface component “S1” is shifted by $0.55 \text{ eV} \pm 0.04 \text{ eV}$ to higher binding energy. The observed shift is typical for Te surface atoms. For example, a surface core level shift of 0.475 eV has been reported for the CdTe(111)B surface.¹⁹ The component “S1” can therefore be assigned to probably unpassivated Te atoms at the nanocrystal surface. Note also that the (111) lattice planes are likely to be representative for a large fraction of the entire nanocrystal surface.²⁰

The component “S2” has a chemical shift of $3.50 \text{ eV} \pm 0.06 \text{ eV}$ toward higher binding energy. It has probably to be assigned to oxidized Te surface atoms. A binding energy of 43.4 eV has for example been reported for the Te $4d_{5/2}$ level in TeO_2 .²¹

In summary, three distinct types of Te sites were observed in the case of the lowly luminescent CdTe nanocrystals. These are Te atoms in the interior of the nanocrystals, Te atoms at the surface, and a small amount of oxidized Te surface atoms. The surface atoms are likely to be unpassivated, because the observed surface core level shift is quite similar to the shift reported for a CdTe(111)B surface.

Te 4d spectra of the highly luminescent CdTe nanocrystals look different and are presented in Figure 9. Part a shows a spectrum recorded at a surface sensitive energy. A fit of a quality comparable to that of the fits in Figure 8 could already be achieved with only one spin-orbit split doublet of Voigt functions. The deficiencies in the residua of the spectra were

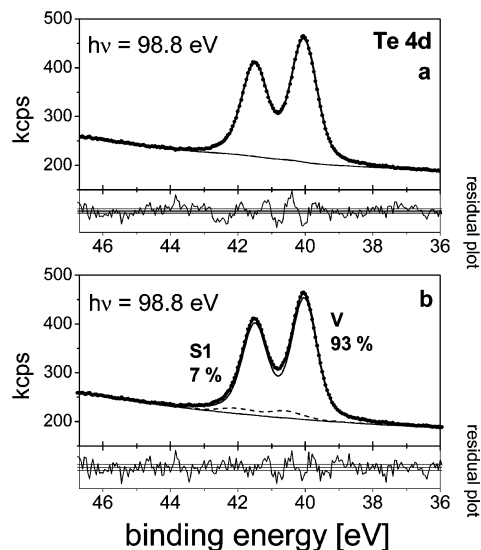


Figure 9. High-resolution Te 4d spectra of the highly luminescent CdTe nanocrystals at a surface sensitive energy fitted with one (a) or two (b) spin-orbit split doublets of Voigt functions.

not pronounced enough for unambiguous determination of a second component here.

However, one can adopt the numerical value for the shift from the study of the lowly luminescent nanocrystals and then fit the spectra of the highly luminescent sample with two components. Figure 9b shows the spectrum (9a) fitted in improved quality with a second component shifted by 0.55 eV. The relative intensity of the component “S1” is much lower than in the case of the lowly luminescent CdTe nanocrystals. The former component “S2” is below the detection limit now. This means that the highly luminescent nanocrystals possess much less surface Te atoms. Since unpassivated surface sites can frequently function as traps²² and give rise to nonradiative recombination, this result may at least partly explain the observed differences in the photoluminescence efficiency. A structural model giving a possible explanation for the formation of a nearly Te-free surface in the case of the highly luminescent CdTe nanocrystals will be suggested later in this article.

4.4. Study of the Te 3d Level. Te 3d spectra yield results similar to those of the 4d spectra. Figure 10a shows a spectrum of the Te $3d_{5/2}$ level of the highly luminescent CdTe nanocrystals recorded at a surface-sensitive energy. There is only one component at a binding energy of 572.8 eV in good agreement with the values reported in CdTe bulk studies.¹⁴ Figure 10b shows the corresponding spectrum of the lowly luminescent CdTe nanocrystals. It clearly comprises three components.

Unambiguous fitting is, however, more difficult than in the case of the 4d level spectra, because the Te 3d level has a much higher binding energy and at higher photon energy the experimental resolution is limited by the increased source width. Therefore, the exact shift and relative intensity of the component labeled “S1” cannot be as precisely determined. Using a literature value of 0.5 eV for the Lorentzian width,²³ we find a shift of 0.88 eV toward higher binding energy. But rather good fits may also be achieved with shifts of only 0.6 eV. The component “S1” can again be attributed to Te atoms at the nanocrystal surface. For example, in a study of Cd(Zn)Te(100), a surface core level shift of 0.93 eV has been observed.²³ The component “S2” has a chemical shift of 3.6 eV toward higher binding energy and can be attributed to oxidized Te surface sites.^{11,21}

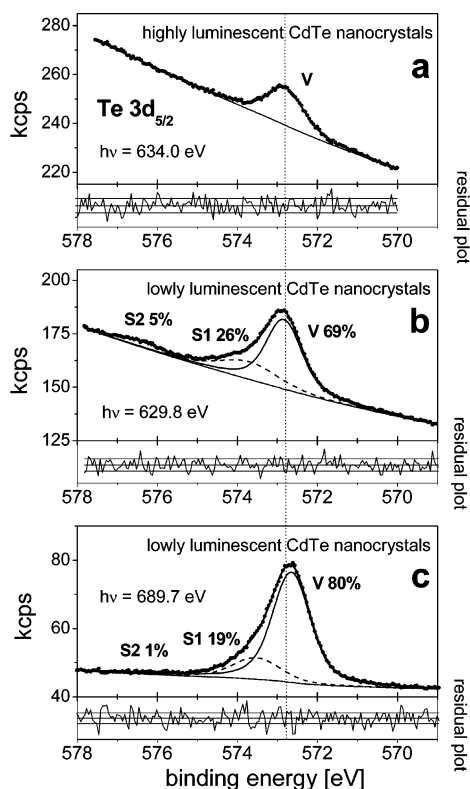


Figure 10. High-resolution Te 3d_{5/2} spectra of the highly (a) and lowly (b,c) luminescent CdTe nanocrystals. The spectra (b) and (c) have been recorded at different excitation energies.

Figure 10c shows a spectrum of the lowly luminescent CdTe nanocrystals recorded at a slightly higher photon energy. To allow an intensity comparison, the shifts of the components “S1” and “S2” were fixed in the presented fit to the values found for the spectrum shown in Figure 10b. The relative intensities have slightly decreased in favor of the component “V”. Thus the attribution of “S1” and “S2” to surface Te atoms is justified.

In summary, the Te 3d spectra support the results of the 4d spectra. In the case of the lowly luminescent CdTe nanocrystals, again three types of Te sites are observed. They can be attributed to Te atoms in the interior of the nanocrystals, atoms at the surface, and to oxidized surface atoms, respectively. In the case of the highly luminescent sample, the surface components are absent. Note, however, that a very small surface component like it was observed for the Te 4d level of the highly luminescent CdTe nanocrystals and is more difficult to detect in the 3d spectra because of the limited experimental resolution and more noisy spectra.

4.5. Study of the S 2p Level. As mentioned in the Experimental Section, the CdTe nanocrystals are capped with thioglycolic acid (TGA). So the study of the S 2p level is in principle of interest, especially because some sulfur atoms originating from the organic stabilizer may have been incorporated into the CdTe lattice during the synthesis.^{2,12} Unfortunately, due to radiation damage in the ligand shell, the analysis of the S 2p spectra turned out to be rather complicated and not conclusive.

S 2p spectra (not shown) have been recorded for both samples and showed three features. One component had a binding energy of about 163.5 eV and probably corresponds to TGA ligands attached to surface Cd sites. Quite similar binding energies have been reported for thiol ligands attached to surface Cd atoms in nanocrystalline CdS.^{4–6} Two additional components were observed around 162.4 and 161.4 eV. Those components might

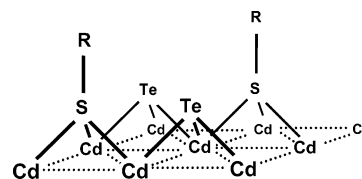


Figure 11. Structure model of a CdTe(111)B surface where some of the surface Te atoms are replaced by TGA (S–R).

be associated with sulfur incorporated into the CdTe lattice, because the S 2p_{3/2} level in CdS has a binding energy of 161.7 eV. But the understanding of the spectra was seriously complicated by a considerable degree of radiation damage. Under irradiation, the sulfur at 162.4 eV was partly transformed into the species at 161.4 eV. It is well-known that radiation damage can easily occur for organic molecules such as thiols adsorbed on gold for example.²⁴ Therefore it is not surprising to observe radiation damage also in the ligand shell of the nanocrystals. In contrast, note again that such radiation damage was not observed for the core levels associated with the proper nanocrystals, i.e., for the Cd and Te core levels. The ligand shell is obviously more fragile with respect to irradiation. A conclusive analysis of the S 2p spectra was therefore not possible here.

5. Discussion of the Surface Structure and the Origin of High Luminescence

The high-resolution photoelectron spectra have revealed as the main difference between the two samples that the lowly luminescent CdTe nanocrystals possess much more Te atoms at the surface than the highly luminescent ones. Since the observed surface core level shift of 0.55 eV is close to the value reported for a CdTe(111)B surface,¹⁹ it is reasonable to assume that a considerable fraction of the surface Te atoms is present in such an environment in the lowly luminescent CdTe nanocrystals. Note also that there were already other reasons to suppose that the (111) lattice planes are representative for a large fraction of the entire nanocrystal surface.²⁰

As illustrated in Figure 11, during the synthesis some of the surface Te sites may be occupied by stabilizer molecules instead of by Te atoms. The occupation of the surface sites by 4-fold coordinated sulfur atoms should result in a more stable structure than the occupation by only 3-fold coordinated Te atoms with dangling bonds. Therefore, the occupation of the surface sites in question by sulfur atoms with an additional bond to the organic rest of the stabilizer should be even favorable from a thermodynamic point of view.

Note the two effects of the occupation of surface sites by S instead of by Te atoms: Such a structure results not only in the removal of dangling bonds of Te atoms from the surface, but moreover leads to the formation of a core–shell like structure. A CdS like surface layer builds a potential wall at the surface of the CdTe nanocrystals which results in a better confinement of photogenerated charge carriers. Both effects would lead to a higher photoluminescence efficiency.

The assumption of such a surface structure is supported by EXAFS investigations of small (1.8 nm diameter) thiol-capped CdTe nanocrystals.²⁵ These investigations showed a strong evidence for Cd–SR bonds near the surface and no indications for the presence of Te atoms at the surface. Hence a structure model of a CdTe nanocrystal covered by a surface layer of Cd–SR was suggested.²⁵

Moreover, our results are consistent with the mentioned photoemission study of Zhang and Yang who have measured

S/Te ratios for 3-mercaptopropionic acid-stabilized CdTe nanocrystals of different photoluminescence efficiencies.¹¹ Higher ratios of S/Te were found for highly luminescent samples. In conclusion, high photoluminescence quantum yields were attributed to the effective passivation by the formation of Cd–thiol complexes at the nanocrystal surface.¹¹

Having good reasons now to assume the partial occupation of surface Te sites by thiol ligands during the synthesis, we can finally address the question of why the preparation of highly luminescent CdTe nanocrystals demands low net growth rates. We would like at least to suggest a possible explanation here. In conclusion, from the above paragraphs high photoluminescence efficiency is caused by the removal of surface Te atoms with dangling bonds in favor of the formation of a Cd–SR surface layer. As discussed above, such structures may furthermore be favorable from a thermodynamic point of view. If the nanocrystals are now grown slowly under conditions of a dynamic equilibrium of growth and dissolution, it is natural that the thermodynamically favorable structure is more likely to be obtained. And this may give an explanation of why the thiol-stabilized CdTe nanocrystals prepared at low net growth rates present the highest photoluminescence efficiencies.

Until now, the exact nature of the surface states providing nonradiative recombination pathways has not been fully clarified. Investigations of organometallically prepared CdTe nanocrystals capped with dodecylamine and trioctylphosphine indicate that mainly oxidized surface Te atoms may be responsible for luminescence quenching.²⁶ In our samples, oxidized Te surface atoms were observed only in the Te 3d and Te 4d spectra of the lowly luminescent CdTe nanocrystals. The occupation of surface Te sites by thiol ligands instead of by Te atoms obviously also prevents the oxidation of Te. Therefore, the above considerations would fully keep their meaning, if luminescence quenching is due to oxidized surface Te atoms.

Another note may be necessary on the possibility of surface reconstruction. Although the observed shift of the component “S1” in the Te 4d spectra is very close to the value reported for a CdTe(111)B surface, we cannot exclude the possibility that the observed component is due to surface reconstruction. Various examples of reconstructed CdTe surfaces have been reported in the literature.^{27–29} As an example, we would like to mention investigations of CdTe(100) surfaces which have indicated that Cd-terminated reconstructions seem to be thermodynamically more stable than Te-terminated reconstructions.²⁹ Under such circumstances, the formation of a nearly Te-free surface should again be more likely in the case of the highly luminescent CdTe nanocrystals prepared slowly in an equilibrium of dissolution and growth.

6. Summary

In summary, our high-resolution photoemission study of TGA-capped CdTe nanocrystals has revealed that the lowly luminescent nanocrystals, prepared under conditions far away from the equilibrium of growth and dissolution, present a considerable amount of surface Te atoms. The surface core level shift observed in the Te 4d spectra points toward a CdTe(111)B surface with unpassivated Te atoms. The dangling bonds at the surface might give rise to nonradiative recombination pathways. Furthermore, the lowly luminescent CdTe nanocrystals present oxidized Te surface sites which are also likely to result in luminescence quenching. In the highly luminescent CdTe

nanocrystals which have been prepared slowly in an equilibrium of growth and dissolution, there are much less Te atoms at the surface. Instead, most of the Te surface sites seem to be occupied by thiol ligands. In principle, sulfur atoms can be present at the surface in 4-fold coordination with three bonds to surface Cd atoms and the last bond to the organic rest of the stabilizer molecule. Since such a structure is also likely to be formed from a thermodynamic point of view, this model may give an explanation of why the highest photoluminescence quantum yields are observed for CdTe nanocrystals prepared slowly in a dynamic equilibrium of dissolution and growth.

Acknowledgment. We thank Dr. A. L. Rogach from the University of Munich for useful discussions. This work was supported by the German Science Foundation (DFG) within the framework of the SFB 508.

References and Notes

- (1) Talapin, D. V.; Rogach, A. L.; Shevchenko, E. V.; Kornowski, A.; Haase, M.; Weller, H. *J. Am. Chem. Soc.* **2002**, *124*, 5782.
- (2) Gaponik, N.; Talapin, D. V.; Rogach, A. L.; Hoppe, K.; Shevchenko, E. V.; Kornowski, A.; Eychmüller, A.; Weller, H. *J. Phys. Chem. B* **2002**, *106*, 7177.
- (3) Seah, M. P.; Dench, W. A. *Surf. Interface Anal.* **1979**, *1*, 2.
- (4) Winkler, U.; Eich, D.; Chen, Z. H.; Fink, R.; Kulkarni, S. K.; Umbach, E. *Phys. Status Solidi A* **1999**, *173*, 253.
- (5) Winkler, U.; Eich, D.; Chen, Z. H.; Fink, R.; Kulkarni, S. K.; Umbach, E. *Chem. Phys. Lett.* **1999**, *306*, 95.
- (6) Nanda, J.; Kuruvilla, B. A.; Sarma, D. D. *Phys. Rev. B* **1999**, *59*, 7473.
- (7) Nanda, J.; Sarma, D. D. *J. Appl. Phys.* **2001**, *90*, 2504.
- (8) Borchert, H.; Talapin, D. V.; McGinley, C.; Adam, S.; Lobo, A.; de Castro, A. R. B.; Möller, T.; Weller, H. *J. Chem. Phys.* **2003**, *119*, 1800.
- (9) McGinley, C.; Riedler, M.; Möller, T.; Borchert, H.; Haubold, S.; Haase, M.; Weller, H. *Phys. Rev. B* **2002**, *65*, 245308.
- (10) Borchert, H.; Dorfs, D.; McGinley, C.; Adam, S.; Möller, T.; Weller, H.; Eychmüller, A. *J. Phys. Chem. B* **2003**, *107*, 7486.
- (11) Zhang, H.; Yang, B. *Thin Solid Films* **2002**, *418*, 169.
- (12) Rogach, A. L. *Mater. Sci. Eng., B* **2000**, *69–70*, 435.
- (13) Rogach, A. L.; Katsikas, L.; Kornowski, A.; Su, D.; Eychmüller, A.; Weller, H. *Ber. Bunsen-Ges. Phys. Chem.* **1996**, *100*, 1772.
- (14) Ricco, A. J.; White, H. S.; Wrighton, M. S. *J. Vac. Sci. Technol. A* **1984**, *2*, 910.
- (15) John, P.; Leible, F. M.; Miller, T.; Hsieh, T. C.; Chiang, T.-C. *Superlattices Microstruct.* **1987**, *3*, 347.
- (16) Prince, K. C.; Paolucci, G.; Chab, V.; Surman, M.; Bradshaw, A. M. *Surf. Sci.* **1988**, *206*, L871.
- (17) John, P.; Miller, T.; Hsieh, T. C.; Shapiro, A. P.; Wachs, A. L.; Chiang, T.-C. *Phys. Rev. B* **1986**, *34*, 6704.
- (18) Ley, L.; Pollak, R. A.; McFeely, F. R.; Kowalczyk, S. P.; Shirley, D. A. *Phys. Rev. B* **1974**, *9*, 600.
- (19) Sporken, R.; Sivananthan, S.; Reno, J.; Faurie, J. P. *J. Vac. Sci. Technol. B* **1988**, *6*, 1204.
- (20) Lu, P.; Smith, D. J. *Phys. Rev. Lett.* **1987**, *59*, 2177.
- (21) Bahl, M. K.; Watson, R. L.; Irgolic, K. J. *J. Chem. Phys.* **1977**, *66*, 5526.
- (22) Gfroerer, T. H. Photoluminescence in Analysis of Surfaces and Interfaces. In *Encyclopedia of Analytical Chemistry*; Meyers, R. A., Ed.; John Wiley & Sons Ltd.: Chichester, 2000; pp 9209–9231.
- (23) Heske, C.; Winkler, U.; Held, G.; Fink, R.; Umbach, E.; Jung, Ch.; Bressler, P. R.; Hellwig, Ch. *Phys. Rev. B* **1997**, *56*, 2070.
- (24) Heister, K.; Zharnikov, M.; Grunze, M.; Johansson, L. S. O.; Ulman, A. *Langmuir* **2001**, *17*, 8.
- (25) Rockenberger, J.; Tröger, L.; Rogach, A. L.; Tischer, M.; Grundmann, M.; Eychmüller, A.; Weller, H. *J. Chem. Phys.* **1998**, *108*, 7807.
- (26) Talapin, D. V.; Haubold, S.; Weller, H. Unpublished results.
- (27) Seehofer, L.; Falkenberg, G.; Johnson, R. L.; Etgens, V. H.; Tatarenko, S.; Brun, D.; Daudin, B. *Appl. Phys. Lett.* **1995**, *67*, 1680.
- (28) Veron, M. B.; Sauvage-Simkin, M.; Etgens, V. H.; Tatarenko, S.; van der Vegt, H. A.; Ferrer, S. *Appl. Phys. Lett.* **1995**, *67*, 3957.
- (29) Heske, C.; Winkler, U.; Neureiter, H.; Sokolowski, M.; Fink, R.; Umbach, E.; Jung, Ch.; Bressler, P. R. *Appl. Phys. Lett.* **1997**, *70*, 1022.